Velocity field on the vicinity of a slot jet impinging a curved wall

By

V.GILARD and L.-E.BRIZZI

Laboratoire d'Etudes Aérodynamiques
(UMR 6609)Boulevard Marie et Pierre Curie, Téléport 2, BP 30179
86960 FUTUROSCOPE CHASSENEUIL Cedex
FRANCE
Tél : (33) 05 49 49 69 27
Fax : (33) 05 49 49 69 68
e-mail : Laurent.Brizzi@lea.univ-poitiers.fr

ABSTRACT

An experimental investigation of aerodynamics of a slot jet impinging a concave wall is presented. So flow visualisations, velocity measurements by PIV and pressure measurements are carried out. The influence of several characteristic parameters of jets impinging a curved wall: (the relative curvature of the wall Dc/b, the impinging height H/b and the Reynolds number Re) is studied. A statistical data processing allows us to obtain the mean velocity fields and the Reynolds stresses. Among the studied parameters, the effect of the relative curvature of the wall is studied in particular because of a jet beating phenomenon observed for the lower relative curvature. This different behaviour is clearly shown on the velocity histograms for the vertical component (cf. figure). Thus three modes characteristic of the flow are observed and described for the lower relative curvature. Finally, the pressure measurements enable to determine a criterion that allows us to know the jet behaviour.
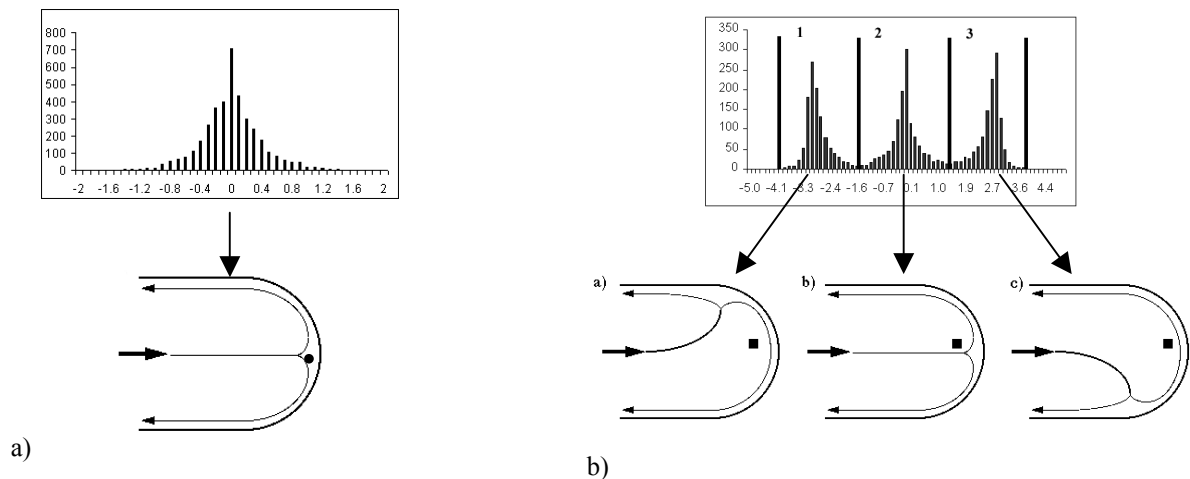
Figure: Velocity histograms for the vertical component (V) and characteristic modes corresponding for (Re_b=3200, H/b=7): a) for Dc/b=9.4 (histogram at the reference point (●) x/b=6.7; y/b=0), b) for Dc/b=5.2 (histogram at the reference point (■) x/b=5.3; y/b=0.7).

INTRODUCTION

One of the means frequently used by the manufacturers of aeroplane engines to cool the turbine blades is the impinging jets technique. With the film cooling technique, this process improves thermal exchanges between walls and fluid. The aim of this technique is to bring a certain quantity of "fresh" air on the engine compressor level and to restore it on the turbine level. This fluid goes inside the blades and is ejected, through several lines of small holes, on the inner part of the blades. By conduction, the heat of the blade is thus "pumped" by the fluid. Because of the low gap between the internal wall of the blade and the holes, we often model this flow by several lines of jets impinging a plane wall. However, for the leading edge of the blade, this assumption (plane wall) is not true : the jets impinge a concave surface.

Also, after many studies on the impinging jets on the wall plane, we have chosen to study the influence of several characteristic parameters of jets impinging a curved wall: the curvature radius, the impact distance, the Reynolds number, etc.

In this field of work, several papers report data on a single jet impinging a curved surface (slot jet: Brahma et al. (1994),Gau & Chung (1991), McDaniel & Webb (2000), Yang et al. (1999) or round jet: Cheng & Wang (1982), Choi et al. (2000), Cornaro et al. (1999), Lee et al. (1999), Yang et al. (1999)) while other papers (less numerous) deal with the multi-jet impingement problem (Brahma et al. (1994), Cheng & Wang (1982), Hrycak (1982), Hrycak (1999), Metzger (1969)).

Though many works concern the thermal aspect of this problem, its dynamic field has not been studied a lot. As the two phenomena can not be totally dissociated, we have undertaken the aerodynamic study of jets impinging on a curved wall. Before studying a more complex case of a line of discrete jets, we initially undertook the study of a slot jet in order to highlight the structure of the impinging jet. It is this study which we will present.

NOMENCLATURE

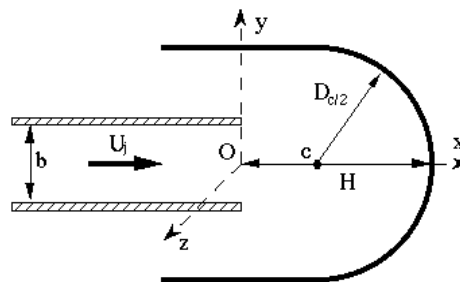|	
b :	Jet height (b=10 mm)
c :	Curvature centre
D_c :	Curvature diameter
H :	Impinging height
L :	Jet width
O :	Jet origin
U,V,W :	Velocity components
U_j :	Jet mean flow velocity

Figure 1 : Test geometry

EXPERIMENTAL APPARATUS

The slot jet is provided by a right-angled parallelepiped channel (955 mm long, 300 mm wide and 10 mm high). Thus, the slot jet is 10 mm high and 300 mm wide. The impingement surface consists of a half cylinder and two plates being used as higher and lower boundaries. All these elements are transparent (Altuglas 4 mm thick) in order to make the visualisations and measurements by LASER velocimetry easier (Figure 1).

The upstream side of the test section (Figure 2) is connected to a fan. A flowmeter and a valve are inserted between the convergent inlet and the fan to regulate and measure the inlet flow rate Q_e.
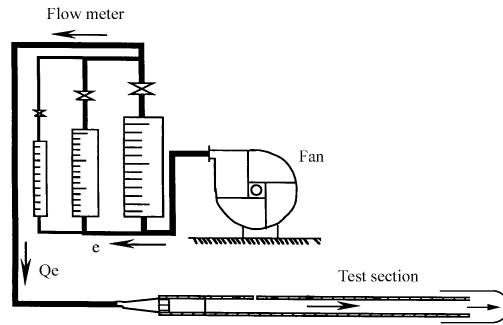
Figure 2 : Experimental device

The three main parameters of this study are :
- ✓ The Reynolds Number based on the jet flow rate Q_e ($Re_b=U_jb/\nu=Q_e/L\nu$). Re_b=1400, 3200 and 6500.
- ✓ The distance between the jet exit and the curved wall (H=30, 50 and 70 mm)
- ✓ The curvature radius (D_c=52 and 94 mm)

VISUALISATION

The flow visualisations were obtained by laser tomography. The flow is seeded by using a smoke generator (water and glycerine) and is highlighted with light sheets issuing from an Argon-Ion LASER. At last, the use of a numerical camera gives the possibility to record some sequences of images with frequencies going up to 1000 frames per second.
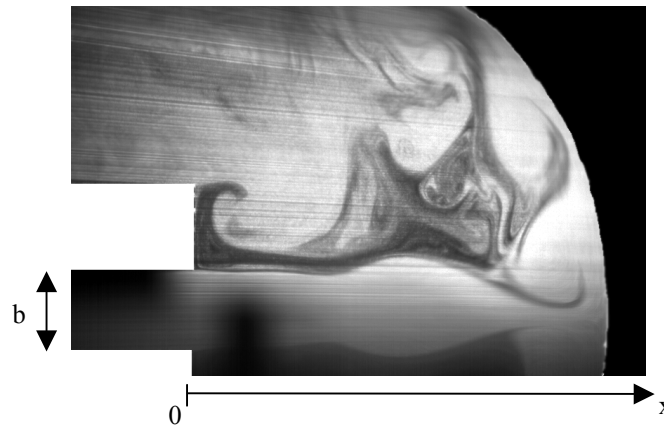

Figure 3: Example of image of a jet impinging a curved wall. (Re_b=1400, H/b=5 Dc/b=9.4)

For technical and symmetry reasons, the flow visualisations were only realised on the higher part of the flow and for several experimental configurations. Figure 3 presents the slot jet impinging the curved wall for the following parameters Re_b=1400, H/b=5 and Dc/b=9.4. On this "snapshot", we observe that the jet, issuing from the left, impacts the curved wall at its centre (x/b=7; y/b=0). Then the flow separates and each part of the jet follows the curved wall, one part downwards and the other one upwards. A vortices formation is also observed in the jet mixing layers. These vortices, characteristic of a shear layer, start to appear as an undulation (starting from x/b=3), and develop in vortices further downstream. Then they impact the wall and are finally convected downstream by the wall jet.

VELOCITY MEASUREMENT BY PIV

The velocity measurements were carried out by the particles imagery velocimetry (PIV) technique. When a LASER illuminates a cross-section of the flow, beforehand seeded with particles, it is possible to visualise two successive moments using a CCD camera. The two successive frames are shifted by a time interval Δt. Then these images are divided into interrogation areas. The average particles displacement $\Delta \vec{d}$ in the corresponding windows is determined by cross-correlation. Thus the mean velocity of the group of particles in each interrogation window is given by the formula: $\vec{V} = \Delta \vec{d} / \Delta t$.

A SPECTRA-PHYSICS Nd-YAG LASER source (2x200 mJ at 10 Hz and 532 nm) is used for measurements with the PIV system (DANTEC Technology) that allows us to obtain several planes of velocity. A LASER beam (wavelength 532 nm) penetrates by the bottom of the test rig by means of the "telescopic arm" ERROL allowing us to illuminate the flow in the plane to observe. Seeding is obtained using a smoke generator (water & glycerin). The mean size of the particles is less than 10 μm.

Pictures are obtained using a Kodak MegaPlus ES 1.0w camera (768x484 pixels double frames) working in cross correlation. The software FlowManager 2.22 pilots the processor Piv2000 which converts pictures into velocity fields.

Measurements are obtained for several experimental configurations. For each configuration, 5000 independent samples of measurement are recorded, divided into 25 packages of 200 recordings. >From an initial velocity field, validation and statistical process are carried out in order to obtain the mean field ($\overline{U}$, $\overline{V}$) and the Reynolds stresses (RMS_u, RMS_v & $\overline{u'v'}$).

To eliminate erroneous measurements during the recording (zones of shade, wall reflections, bad seeding), the data are filtered in each point of measurement, for each acquisition and each velocity component. Thus each sample of measurement is validated according to several criteria. Then the data processing is carried out in two steps.

In the first processing, each sample is validated according to a significant value of the signal/noise ratio (the threshold is fixed here at 2). This one corresponds to the signal/noise ratio between the first and the second peak of the correlation function used for the determination of the velocity. Then starting from these validated values, a velocity histogram at each point and for each velocity component is built, smoothed and then thresholded. So the mean and fluctuating values of the velocity are estimated ($\overline{U}$ and RMS).

In the second processing, the initial measurements are again filtered with a lower threshold than the first processing, (signal/noise ratio at 1.5). Measurements are then filtered by bandwidth re-using the results of the first processing. Supposing that the velocity histogram is Gaussian, only the values included in the interval ($\overline{U} \pm K * RMS$) are validated. K is the confidence level, equal to 3. The mean values and the fluctuations for each velocity component and each point are finally calculated. After the post processing, only the statistics with more than 3000 validated vectors are retained.

Measurement precision has been estimated to be less than 1%, and the maximum bias at 3% for the mean values and at 6% for the RMS values. These include the accuracy, the statistical bias and the position uncertainty. Most of the measurements are realized in and around the symmetry plane (X=0) of the slot jet for all the configurations.

RESULTS

The figure 4 is the mean velocity field obtained by PIV for the following parameters (Re_b=3200; H/b=7; D_c/b=9.4). We observe the jet issuing from the left impacting the centre of the curved wall in x/b=7 and y/b=0. At this location, the flow separates in two. Each part of the fluid skirts the curved wall and arises symmetrical, compared to the horizontal axis on the top and bottom of the figure. We thus observe clearly an impact on the curved wall. In this configuration, RMS values of the horizontal component (U) have a rather particular form: the maximum values ($\approx$1.4 m/s) are reached in the vicinity of the jet shear layer. These two areas located symmetrically to the X-axis meet in the vicinity of the stagnation point and form a horseshoe shape (cf. Figure 4). For the vertical component (V), the intensity of the maximums of the fluctuations is almost identical to that of the horizontal component ($\approx$1.2 m/s). On the other hand, the location of these maximums is different: it is close to near the impact point (x/b=7; y/b=0).

For this configuration, we note that, for several aspects, this behaviour is similar to that observed in the case of a single jet impinging a plane wall. It is not the same when the wall curvature radius is modified.
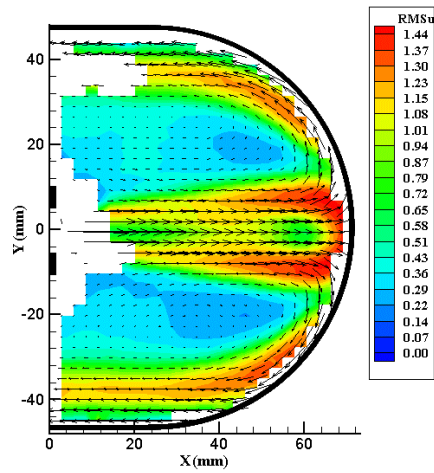
Figure 4 : Mean velocity field and RMS$_u$ values (Re$_b$=3200; Z/b=7; D$_c$/b=9.4).

The figure 5 is the mean velocity field obtained by the PIV for the following parameters (Re$_b$=3200; H/b=7; D$_c$/b=5.2). We observe now that the jet issuing from the left does not impact directly the centre of the curved wall (x/b=7 and y/b=0). Indeed, there is a triangular form area in the vicinity of this impact point where the velocities are very low. The mean flow is always symmetrical compared to the x-axis, but there seems to be a "dead fluid" area which prevents the jet from coming into impact with the curved wall. Thus, the fluid makes a half-turn and comes out, like previously, at the top and bottom of the figure. On the graphs of the fluctuations of the horizontal and vertical velocities, we also observe many modifications. For the horizontal component (RMS$_u$), the position and values of the maximums evolve considerably.
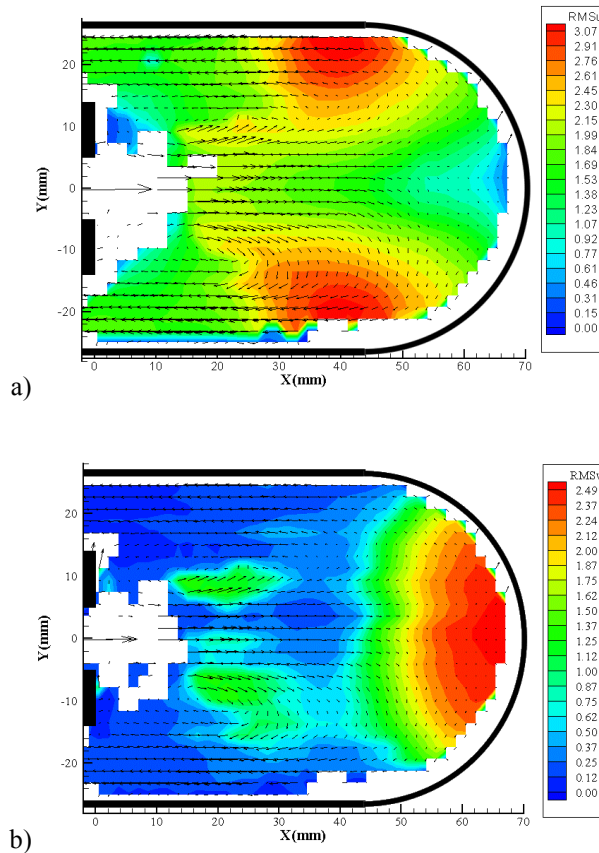

a)

b)

Figure 5 : Mean velocity field and a) RMS$_u$ values, and b) RMS$_v$ values. (Re$_b$=3200; Z/b=7; D$_c$/b=5.2).

5

On the figure 5a, there are two zones with a high intensity ($\approx$3.2 m/s) located symmetrically to the jet axis in x/b=4.5 and y/b=±2.5. For the vertical component (cf. Figure 5b), we find the same behaviour as that of the preceding configuration (Large curvature radius): Only a single zone of maximum in the vicinity of x/b=7 and y/b=0. However, we can notice that the level reached for this new configuration ($\approx$2.49 m/s) is much higher than the precedent. At first sight, this behaviour can appear surprising since there is no impact in x/b=7 and y/b=0 in the case of the small relative curvature.

In the case of the small relative curvature (D_c/b=5.2), the fact that the jet does not impact the centre of the curved wall is a rather surprising phenomenon. Thus in order to understand this different behaviour between the two radius of curvature, the velocity histogram, for a point located in the zone of strong RMSv values, is built for each curvature radius and for the same Reynolds number and imping height. Figure 6 presents the histograms of the vertical component of the velocity for the configuration Re=3200, H/b=7 and for Dc/b=9.4 (figure 6-a) and Dc/b=5.2 (figure 6-b). The velocity histograms are built at the reference points (x/b=6.7; y/b=0) for Dc/b=9.4 and (x/b=5.3; y/b=0.7) for Dc/b=5.2
For the higher relative curvature (Dc/b=9.4), we observe that the velocity histogram has only one peak centred around the value 0 m/s. For this configuration, we saw previously that the jet comes to impact the centre of the wall. The flow has whereas only one direction along the vertical axis and thus only one peak for the vertical component of the velocity.
For the smaller relative curvature (Dc/b=5.2), the histogram shows three distinct peaks centred around the values: -3 m/s, 0 m/s and 2.86 m/s. It can be considered that it is the superposition of three distinct behaviours. In order to study separately these three behaviours, we define three velocity intervals: [-4 ; -1.5 m/s] (mode 1), [±1.5 m/s] (mode 2) and [1.5 ; 4 m/s] (mode 3).
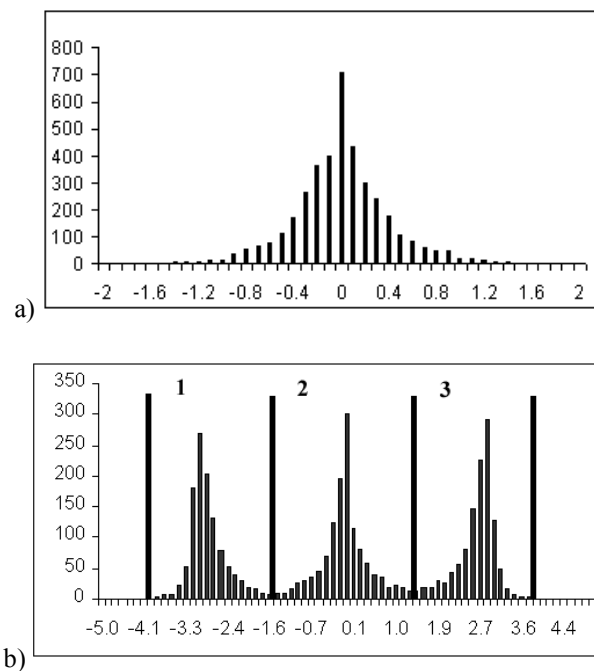

Figure 6 : Velocity histograms for the vertical component (V) (Re$_b$=3200, H/b=7) :
a) for Dc/b=9.4 and at the reference point (x/b=6.7; y/b=0).
b) for Dc/b=5.2 and at the reference point (x/b=5.3; y/b=0.7).

The mean velocity and RMS values of the two components are then recomputed by keeping only the velocity fields for which, at the reference point, the measurement of the vertical velocity component is included in one of the three intervals. The same filtering as previously used is used to calculate the averages for the velocity fields selected. Then, the three flows with different characteristics from the complete velocity field are observed. Figure 7 presents the scheme of flow of the various modes for the configuration Dc/b=5.2.

For mode 1 (figure 7-a), we observe that the jet comes to impact the higher wall of surface and separates then in two parts. A significant part of the jet skirts the curved wall to the bottom and another smaller part sets out again directly towards the left.

For mode 2 (figure 7-b), we notice that the jet comes to impact the wall in its centre. The jet separates and then each part skirts the curved wall on both sides of the stagnation point. We finds here the same flow behaviour that the high relative curvature.

Lastly, for mode 3 (figure 7-c), we observe as for mode 1 that the jet comes to impact the curved wall but here on its lower part, then the jet separates. This time, most of the jet also skirts curved wall upwards and a small part sets out again directly towards the left.

These three flow patterns show clearly the presence of a jet beating from the top to the bottom (mode 1 to 3) and conversely.
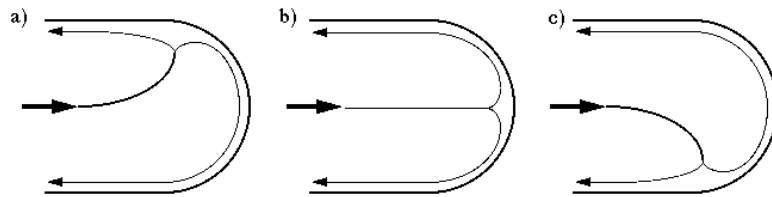

Figure 7: Scheme of the flow

PRESSURE MEASUREMENT

Measurements of pressures in the curved wall are then carried out. So pressure taps (0.4 mm) were created at different locations on the curved wall. For the pressure measurements, differential pressure sensors are connected to an acquisition card and the signal is amplified beforehand. The sampling rate is set at 500 HZ and the time of acquisition is about 10 seconds. The measurements allow us to calculate the pressure coefficient: $C_p = \dfrac{p_i - p_{ref}}{\frac{1}{2}\rho U_j^2}$, where p_i is the static pressure at the tap number i and p_{ref} the pressure reference (here $p_{ref}=p_{atm}$).
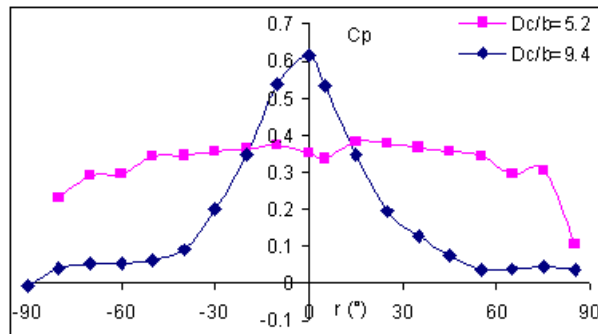

Figure 8: Pressure distribution. (Re_b=3200, H/b=7)

The figure 8, shows the evolution of the pressure coefficient C_P for the two configurations.

For the large radius, the curve is the same as that for a plane wall: the maximum is reached at the stagnation point and a symmetrical decrease is observe on each side of the curve from this point. This pressure maximum confirms the impact of the jet in the centre of the wall.

For the small radius, the curve has a different shape. We do not observe any distinct maximum but rather a constant value on most of the profile, indicating a uniform zone of pressure. In this case, the lack of the maximum pressure coefficient reaffirms that the jet does not impact the centre of the wall. Thus this uniform zone of pressure indicates the presence of the jet beating.

We thus observe if the jet comes to impact the centre of the wall, the pressure coefficient is at the maximum in the centre and that if the jet beats, the pressure coefficient does not have a maximum and is constant along the wall. So the value of the pressure coefficient in the centre of the wall makes it possible to know if the jet impacts the wall or if it beats. A maximum value of pressure coefficient in the centre of the wall is a criterion of the impact.

CONCLUSION

This study on a plane jet impinging a curved wall was carried out according to several parameters (Reynolds number Re, height of H/b impact, relative curve of the wall of Dc/b impact). The velocity measurements by PIV and pressure measurements showed the importance of the relative curvature effect on the jet structure. Thus the effect of relative curvature acts mainly on the jet flow behaviour. Indeed, for a low relative curvature, the flow oscillates around three different modes, then modifying considerably the impinging jet aerodynamic. This modification of the flow will involve certainly a variation of the thermal transfers in the vicinity of the leading edge of the blade. The knowledge of the jet behaviour will make it possible to optimize the blade cooling. In addition, the pressure measurements have confirmed the relative curvature effect and allowed us to know the behaviour of the jet. So, a study of the instability, in the form of beat, could be carried out according to the other parameters.

REFERENCES

BRAHMA, PADHY & PRADHAM : "Experimental studies of heat transfer by slot jet and single/triple row of round jets impinging on semi-cylindrical concave surfaces". Heat Transfer Engineering, vol.15 n°4, pp 66-74, (1994).

CHENG & WANG : "Experimental investigation of heat transfer by single and triple row round jets impinging on semi-cylindrical concave surfaces". Proceeding 7th International Heat Transfer Conference, pp 337-342, (1982).

CHOI, YOO,YANG &LEE: "Measurement of impinging jet flow and heat transfer on a semi-circular concave surface". Journal of Heat and Mass Transfer, vol.43 n°10, pp 1811-1822, (2000).

CORNARO, FLEISCHER & GOLDSTEIN : "Flow visualisation of a round jet impinging on cylindrical surfaces". Experimental Thermal and Fluid Science, vol.20 n°2, pp 66-78, (1999).

GAU & CHUNG : "Surface curvature effect on slot-air-jet impingement cooling flow and heat transfer process". Journal of Heat Transfer Transactions of ASME, vol.113, pp 858-864, (1991).

HRYCAK : "Heat transfer and flow characteristics of jets impinging on a concave hemispherical plate". 7th Int. Heat Transfer Conference Munich, pp 357-362, (1982).

HRYCAK : "Heat transfer from a row of impinging jets to concave cylindrical surfaces". Journal of Heat and Mass Transfer, vol.24, pp 407-419, (1981).

LEE, CHUNG & WON : "The effect of concave surface curvature on heat transfer from a fully developed round impinging jet". Journal of Heat and Mass Transfer, vol.42, pp 2489-2497, (1999).

McDANIEL & WEBB : "Slot jet impingement heat transfer from circular cylinders". Journal of Heat and Mass Transfer, vol.43, pp 1975-7985, (2000).

METZGER, YAMASHITA & JENKINS: "Impingement cooling of concave surfaces with lines of circular air jets", J. of Eng. and Power, pp. 149-158, (1969).

YANG,CHOI & LEE: "An experimental study of slot jet impingement cooling on concave surface : effects of nozzle configuration and curvature". Journal of Heat and Mass Transfer, vol.42, pp 2199-2209, (1999).

YANG, CHANG, SU & HWANG: "Heat transfer of confined impinging jet onto spherically concave surface with piston cooling application". JSME International journal serie B, Fluid and thermal engineering, vol.42, pp 238-248, (1999).